MINERALOGICAL MAPS OF MARS FROM HAPKE MODELING AND SPECTRAL UNMIXING

Mirza Arnaut, Kay Wohlfarth, Arne Grumpe, Christian Wöhler, Image Analysis Group TU Dortmund, Germany
{mirza.arnaut, kay.wohlfarth, arne.grumpe, christian.woehler}@tu-dortmund.de

Introduction: The CRISM instrument [1] onboard the Mars Reconnaissance Orbiter (MRO) was designed to analyze the Martian mineralogy in view of past and present traces of water. The measured radiance spectra, which emerge from the Martian surface, are essentially a nonlinear superposition of the reflectance spectra of Martian endmember minerals. In order to analyze the mineralogical composition of planetary surfaces, spectral unmixing can be employed which disentangles the components and allows for the generation of mineralogical maps. Several works [2,3,4], performed spectral unmixing of regolith analogues and planetary surfaces relying on Hapke's reflectance model [5] which transforms the nonlinear mixing problem of radiance measurements into a simple linear mixing problem of single scattering albedos. In this work, we extend the Hapke-based unmixing procedure of CRISM data in [4] which only analyzes single pixels. As an extension, we generate full mineralogical maps of selected regions. Different to [4], we employ image endmembers which are sampled at the same locations as the CRISM spectra library [6] to make sure we use endmembers present on Mars. The results are discussed in view of plausibility to assess the viability of the described approach and possible further improvements.

Methods: The unmixing technique is partly based on our previous approach [3] for lunar analog materials and the method described in [4]. The radiance mixing of regolith particles is a nonlinear process. Using Hapke's anisotropic multiple-scattering approximation (AMSA)-reflectance model [5], radiance measurements are converted to single scattering albedo, which can be described by a linear mixing law. All in all, the method comprises the following six steps:

Data reduction is carried out based on the thermal emission present in the TIR spectra and redundant spectral layers. To avoid the influence of thermal radiation, the unmixing process has been performed in the spectral range 1 – 2.5 µm. This range minimizes the effects while still conserving the relevant data for the processing.

Preprocessing is performed by using the Integrated Software for Imagers and Spectrometers (ISIS3) [7] to generate a map-projection of the region of interest, which is co-registered to the HRSC - MOLA blend digital topography maps [8].

Atmospheric Correction is crucial since CO_2 in the atmosphere leads to strong absorption bands around 1.4 µm and 2 µm. These absorption bands might erroneously be interpreted as mineral-related absorption features which would disturb the unmixing result. We corrected the CRISM data for atmospheric influences by applying the empiric volcano scan method [6] to the CRISM calibration data record (CRD) [1].

Topographic Normalization and Refinement is performed to exclude topographic variations as the source of radiance changes. Because the HRSC - MOLA blend DTM [8] has a lower resolution compared to CRISM the shape from shading method [9] is carried out to refine the DTM, using a single spectral channel for inducing detailed DTM data.

Albedo extraction is done by employing a nonlinear optimization method which inverts the Hapke model. Albedo spectra are acquired for every pixel in the scene under investigation as well as for specific sites which contain the endmembers as used for the CRISM spectra library [6].

Linear unmixing is performed using a constrained method, which incorporates the non-negativity but also the standard full-additivity requirement of the components. This is achieved by an iterative method and is based on the work of Coleman and Li [10].

Results: The dscribed framework has been applied to two regions: South-west of Melas Chasma [Image ID: 00013F5B] and the northern rim of the crater Nicholso [Image ID: 0000B73D]. The first region is the same as in [4] and was investigated for the purpose of comparison, whereas the second is a typical basalt-rich region.

South-West Melas Chasma was among the top eight landing site candidates for the Mars Rover 2020 mission since hydrated sulfates have been found in past research, e.g., [4], where comparable results were achieved. Besides monohydrated sulfates and bassanite, we found high-Ca pyroxene (hcp) and plagioclase, which are the main components of basaltic rocks. The spatial distribution of the four most abundant minerals is shown in the maps in Fig. 1.

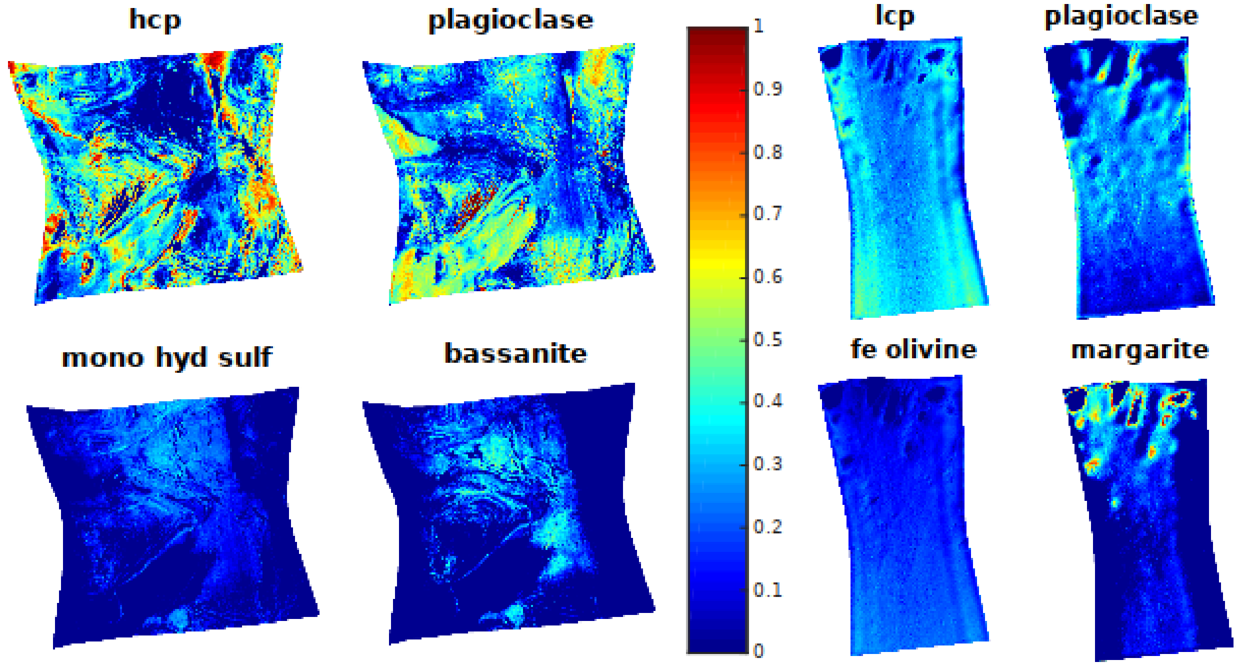

Figure 1: Fractional abundances of the four most frequent endmembers found in *South-West Melas Chasma (left) and the northern rim of the crater Nicholson (right).*

The crater Nicholson is located close to the equator and shows fluvial structures which may indicate past presence of water [11,12]. The presented method has led to reasonable results, since a high abundance of low-Ca pyroxene, plagioclase and iron olivine have been found, which is again typical of basaltic rocks. Some anomalies can be noticed, which are most likely caused by the lack of "spectral smile" correction of the raw data.

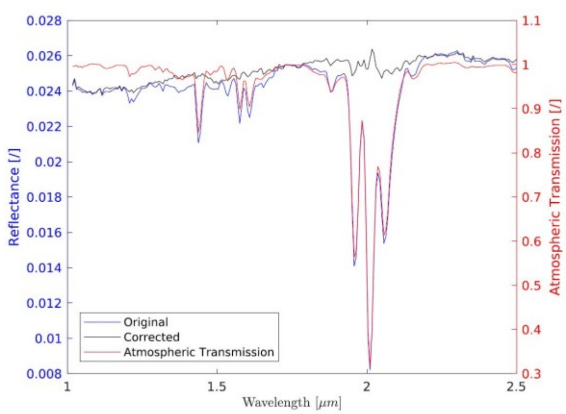

Figure 2: Reflectance spectrum at the crater Nicholson with and without correction of atmospheric effects.

Additionally, the inferred mineral abundances still seem to exhibit a slight dependency on topography, which needs to be compensated for in future analyses. The atmospheric correction method could not fully remove the parasitic effects and some residual small spikes remain (Fig. 2).

Conclusion: A framework has been constructed for unmixing of hyperspectral CRISM data in the range of 1 – 2.5 µm. This enables the construction of mineralogical maps of the Martian surface based on image endmembers. The unmixing results are plausible and consistent with previous studies. To further improve the method, spectral smile compensation, a more refined topographic compensation and validation with in-situ rover measurements are needed.

References: [1] Murchie S. et al. (2007), JGR Planets, 112, E05S03. [2] Hieroi, T. and Pieters, C. (1994) JGR Planets, 99, 10867-10879. [3] Rommel, D. et al. (2017), Icarus, 284, 126-149. [4] Liu, Y. et al. (2016) JGR Planets, 121, 2004-2036. [5] Hapke, B. (2012), Cambridge University Press. [6] Viviano-Beck, C. E., et al. (2014), JGR Planets, 119, 1403–1431. [6] McGuire, P.C. et al. (2009), Planetary and Space Science, 57, 809-815. [7] Anderson J. A. (2004), LPSC XXXV, Abstract #2039. [8] Fergason, R. L et al. (2018), Astrogeology PDS Annex, U. S. [9] Wöhler, C. et al. (2017), ISPRS, XLII-3/W1, 163-170. [10] Coleman, T. and Li, Y. (1996), SIAM Journal on Optimization, 6, 1040-1058. [11] Neukum, G. et al. (2007), LPSC XXXVIII, 1338, 2271. [12] Rommel, D. (2008) Diplomarbeit (Master Thesis), unpublished